applied sciences

MDPI

Article

Impact of Silica Sand on Mechanical Properties of Epoxy Resin Composites and Their Application in CFRP–Concrete Bonding

Riad Babba [1], Kamel Hebbache [2], Abdellah Douadi [2], Mourad Boutlikht [2], Redha Hammouche [3], Saci Dahmani [1,4], Giulia Del Serrone [5] and Laura Moretti [5,*]

1 Faculty of Science and Technology, University of Tamanghasset, Tamanghasset 11001, Algeria
2 Civil Engineering Research Laboratory of Sétif (LRGCS), Department of Civil Engineering, Ferhat Abbas University of Sétif 1, Sétif 19000, Algeria; hebbache.kamel@univ-setif.dz (K.H.)
3 Materials and Durability of Construction Laboratory, Department of Civil Engineering, Faculty of Science and Technology, Frére Mentouri University of Constantine 1, Constantine 25000, Algeria
4 Laboratory of Exploitation and Valorization on Natural Resources in Arid Zones (EVRNZA), University Kasdi Merbah, Ouargla 30000, Algeria
5 Department of Civil, Building, and Environmental Engineering, Sapienza University of Rome, Via Eudossiana 18, 00184 Rome, Italy; giulia.delserrone@uniroma1.it
* Correspondence: laura.moretti@uniroma1.it

Abstract: Premature debonding between carbon fiber-reinforced polymer (CFRP) and concrete is a critical issue in structural reinforcement applications, often leading to a significant reduction in the load-carrying capacity of the system. This failure mode is typically initiated by inadequate adhesion at the interface, compromising the effectiveness of CFRP in enhancing the structural performance of concrete elements. To address these issues, this study explores the impact of silica sand on the mechanical and adhesion properties of epoxy resin composites. Initially, this paper investigates the physical and mechanical properties of epoxy resin composites by varying the ratios of silica sand from 0% to 15% by volume. Subsequently, it examines the effectiveness of these composites as sealing materials to enhance the bond strength between CFRP and concrete. Incorporating a 10% silica content improves the mechanical properties of the epoxy resin, with the tensile strength increasing from 29.47 MPa to 35.52 MPa and an elastic modulus from 4.38 GPa to 5.83 GPa. Furthermore, silica sand enhances the adhesion strength between CFRP and concrete, as confirmed by the increase in the pull-out force from 14.21 kN to 18.79 kN. Silica particles improve surface roughness and interlocking, contributing to a better load distribution and stress transfer at the interface. Therefore, silica-filled epoxy resin is an efficient material for CFRP–concrete bonding applications.

Keywords: epoxy resin; silica sand; CFRP–concrete bonding; pull-out force; structural reinforcement

Citation: Babba, R.; Hebbache, K.; Douadi, A.; Boutlikht, M.; Hammouche, R.; Dahmani, S.; Del Serrone, G.; Moretti, L. Impact of Silica Sand on Mechanical Properties of Epoxy Resin Composites and Their Application in CFRP–Concrete Bonding. *Appl. Sci.* **2024**, *14*, 6599. https://doi.org/10.3390/app14156599

Academic Editor: Chao-Wei Tang

Received: 1 July 2024
Revised: 23 July 2024
Accepted: 26 July 2024
Published: 28 July 2024

1. Introduction

In recent decades, the interest in developing effective repair and reinforcement methods to prolong the concrete structure service life has been increasing. Recent advancements in materials science have underscored the potential of composite materials, particularly carbon fiber-reinforced polymer (CFRP), for the reinforcement and repair of concrete structures [1,2]. CFRP is especially valued for its high strength-to-weight ratio, corrosion resistance, and ease of application, making it an ideal candidate for structural enhancement [3]. Among the various techniques for reinforcing concrete structures with CFRP, the Near-Surface Mounted (NSM) method stands out [4]. This method involves embedding CFRP rods or strips into pre-cut grooves on the concrete surface and securing them with adhesives, typically epoxy resins. The effectiveness of the NSM method is highly dependent on the bond strength between the CFRP and the concrete, facilitated by the adhesive used. Extensive research has been conducted on the bond performance of CFRP systems using different types of adhesives. Capozucca [3] discussed the implications of

reinforcement corrosion on concrete integrity, emphasizing the need for durable repair solutions. Al-Mahmoud et al. [5] and Parretti et al. [6] demonstrated the advantages of using CFRP for structural reinforcement, noting the NSM method's significant enhancement of concrete structures' mechanical performance. Chen et al. [7] further elaborated on the challenges of preliminary debonding in bonded reinforcement systems and highlighted the NSM technique's potential to address these issues. The bond strength between the CFRP and concrete is crucial for the long-term performance and durability of repaired structures. Researchers have examined various parameters affecting this bond, such as the type of adhesive [8–10], curing conditions, and surface preparation of the CFRP and concrete [11,12]. For instance, Shield et al. [13], Sharaky et al. [14], and Lee et al. [15] explored the impact of different adhesives on bond strength, concluding that the adhesive's mechanical properties and its interaction with the concrete surface significantly influence the overall bond performance. The epoxy resin transfers shear stresses between concrete and the composite reinforcement [16]. This parameter affects the behavior and long-term durability of concrete structures undergoing repair through the NSM technique [17,18]. Table 1 provides a general overview of recent studies related to the NSM technique.

Table 1. Summary of recent research related to NSM techniques.

Reference	Adhesive	Main Results
Shield et al. [13]	Seven types of adhesives	Significant variations in bond strength and failure mechanisms among epoxy adhesives.
Sharaky et al. [14]	Four types of epoxy resins	Enhanced bond capacity and ductility with more ductile adhesives.
Lee et al. [15]	Seven adhesive types	Increased bond strength with higher material bond strength adhesives.
Benedetti et al. [19]	One type of epoxy resin	Elevated curing temperature accelerates curing and bond performance.
Al-Saadi et al. [20]	One type of epoxy adhesive	Surface conditions of CFRP strips significantly affect bond strength and behavior.
Mohammed et al. [21]	Innovative high-strength self-compacting cementitious adhesive (IHSSC-CA)	IHSSC-CA improves bond performance at high temperatures due to better load transfer and composite action.
Rahman et al. [22]	Partial replacement of epoxy with cement mortar	Cement mortar with NSM steel bars is a cost-effective alternative for enhancing the flexural performance of RC beams with NSM steel bars.
Torres et al. [23]	Three epoxy types	Properties of epoxy play a crucial role in the bond performance of NSM FRP strengthening.
Mohammed et al. [24]	IHSSC-CA	A smooth surface of the adhesive layer prevents localized brittle failure in the concrete.
Al-Saadi et al. [25]	IHSSC-CA	IHSSC-CA improves the bond strength, stiffness, ductility, and residual strength of the NSM CFRP system.
Cruz et al. [26]	Two types of stiff adhesives and one flexible adhesive	Stiff adhesives show maximum pullout force and bond stiffness higher than flexible adhesives.
Mohammadi et al. [27]	Two classes of cement-based adhesives	Cement-based adhesives exhibit great potential for bonding NSM CFRP systems in reinforced concrete structures.

Based on the literature, all studies on the bond between CFRP and concrete using the Near-Surface Mounted (NSM) method have utilized either non-loaded epoxy resin or special cement as a sealing material between the concrete and reinforcement. These approaches inherently suffer from premature failure at the reinforcement–resin or resin–concrete interfaces. Additionally, while several studies have investigated the mechanical

and thermal properties of resins with mineral charges such as kaolin and sand glass powder, refs. [28–31] none have explored the application of these loaded resins in the context of CFRP applications. This study addresses this gap by incorporating silica sand as a filler material in epoxy resin composites to enhance the frictional forces and improve the adhesion efficiency between CFRP and concrete in the NSM method. This innovative approach not only aims to mitigate premature failure issues, but also seeks to enhance the mechanical and thermal properties of the composite material, thus providing new perspectives for more efficient and durable applications in structural reinforcement. By exploring the use of silica sand-loaded epoxy resin in CFRP applications, this study opens new perspectives on improving the performance and reliability of structural reinforcement techniques. This innovative approach could pave the way for more efficient and durable solutions in the field of civil engineering.

2. Material and Method

The silica sand used in this study was sourced from the Tlemcen region in northwest Algeria, renowned for its high silica content and well-defined granulometry, with particle sizes ranging from 0 to 5 mm. Fourier Transform Infrared Spectroscopy (FTIR) was applied using a Shimadzu FTIR 8400 spectrometer (Shimadzu Corporation, Kyoto, Japan) to assess its functional groups (Figure 1).

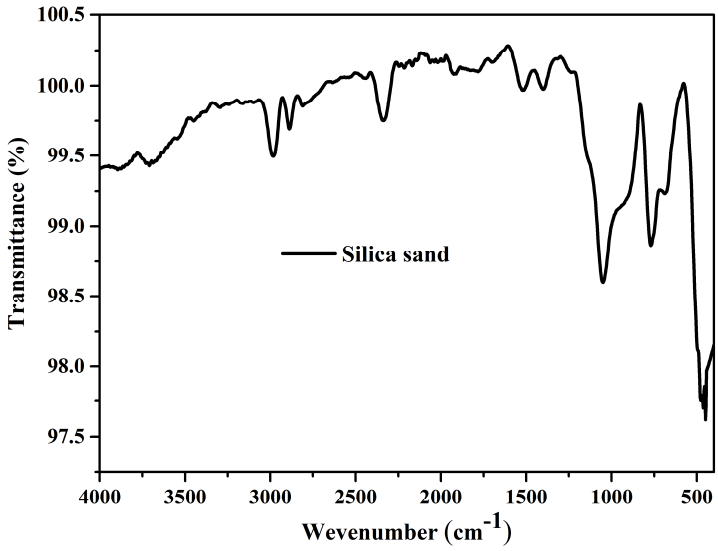

Figure 1. Absorption spectrum of silica sand.

The FTIR spectrum of the sand reveals that the prevailing chemical bonds consist of Si-O (Table 2).

Table 2. The main bands of IR.

Frequency (cm^{-1})	Vibration Kind
458.68	Si-O-Si
684.36	Si-O vibration
767.89	Si-O
1051.53	Stretching vibrations Si-O-Si
1689; 1800; 3700	Stretching H-OH

Particle size analysis was performed using a Mastersizer 2000 laser analyzer (Malvern Instruments, Malvern, UK) and the scanning electron microscope "SEM" Philips/FEI XL 30S FEG Chatsworth, CA, USA. The morphology of silica sand grains showcases angular shapes (Figure 2). Figure 3 shows an almost homogeneous size distribution of silica sand.

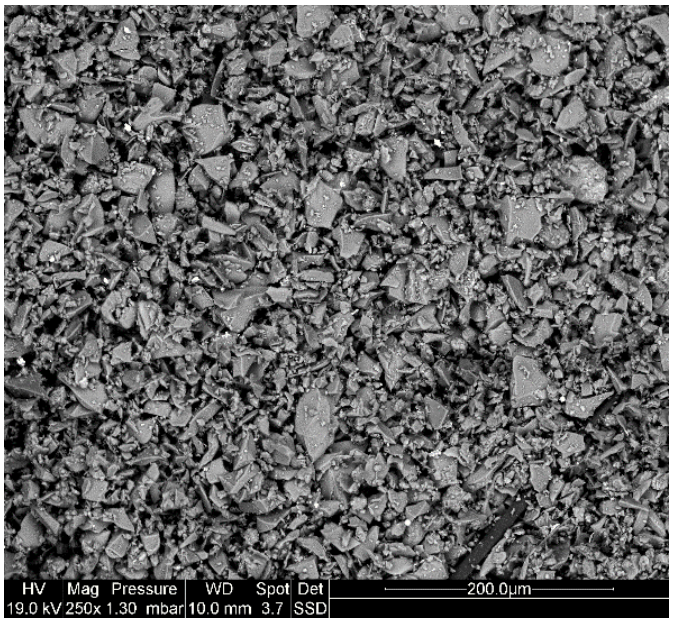

Figure 2. Particle shape of silica sand grains.

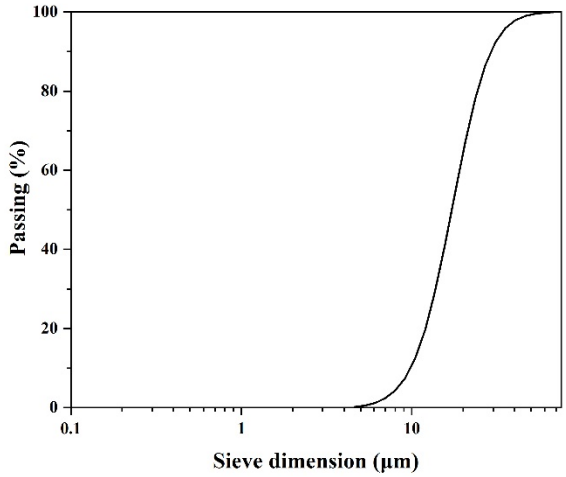

Figure 3. Particle size distribution of silica sand.

The chemical composition of the materials was determined using X-ray fluorescence spectroscopy (Table 3).

Table 3. Chemical properties of the used crushed sand.

Compound	SiO_2	Al_2O_3	Fe_2O_3	CaO	MgO	K_2O	Na_2O	SO_3	L.O.I. (%)
(%)	98.91	-	0.5	0.52	-	-	-	-	0.02

The epoxy resin selected for this study was a two-component, high-performance adhesive comprising a resin (part A) and a hardener (part B) mixed in a 4:1 ratio. Table 4 lists its properties. The properties of the resin presented in Table 4 are obtained from the technical data sheet (https://dza.sika.com/ accessed on 8 June 2024).

Table 4. Properties of the epoxy resin.

Density (kg/L)	Tensile Strength (MPa)	Young's Modulus (MPa)	Elongation at Break (%)	Glass Transition Temperature (°C)
1.3	30	4500	9	73.5

The composite synthesis involves a sequential blending process to ensure optimal filler incorporation. Table 5 lists the percentage of silica filler added to the composite, ranging from 0% to 15% by volume. These proportions are based on the total volume of the epoxy resin system (A + B), allowing for a detailed analysis of their impact on the composite properties.

Table 5. Percentage of sand added to the resin.

Mixture Type	Mixture 1	Mixture 2	Mixture 3	Mixture 4
Filler ratio	Resin + 0%	Resin + 5%	Resin + 10%	Resin + 15%

The density of the composite materials was determined using the hydrostatic weighing method according to the NF T 51-561 standard [32]. Density measurements were obtained by averaging the results from three samples, each subjected to double weighing at 22 °C Equation (1):

$$\rho = \frac{\rho_e \times m_r}{m_r - \left(m_f - m_p\right)} \quad (1)$$

where ρ and ρ_e are the densities of the sample and the immersion liquid (water), respectively, and m_r, m_f, and m_p are the sample's mass in air, the mass of the test tube with the sample holder, and the mass of the test tube holder in water, respectively.

Unfilled (Mixture 1, without silica sand) and filled resin composite samples (Mixtures 2, 3, and 4, with silica sand) were prepared to investigate their mechanical properties. Tensile tests according to the ISO 527-2 standard [33] returned the elastic modulus, ultimate tensile strength, and elongation at break. Silicone molds ensured high-quality specimens with minimal defects (Figure 4).

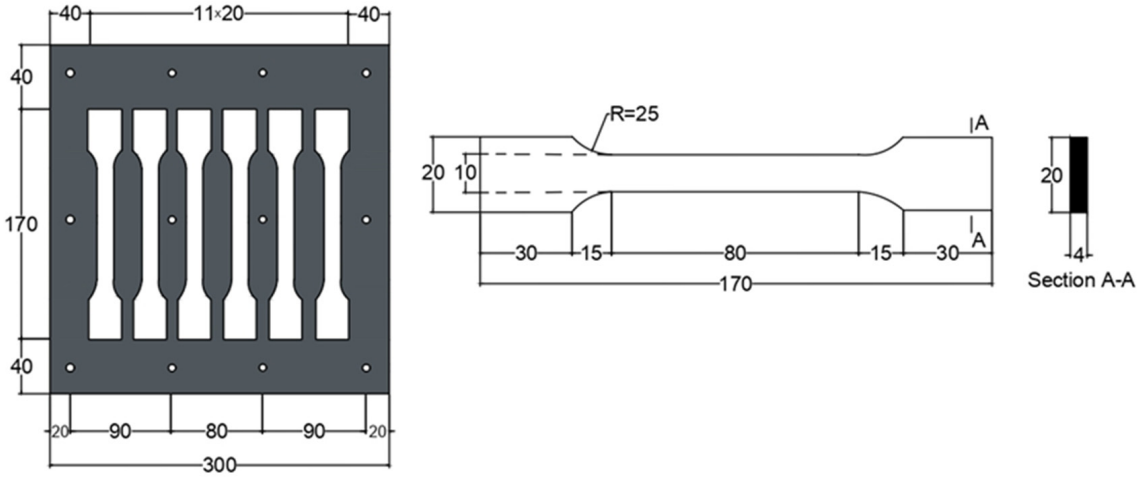

Figure 4. Geometry and dimensions of the molds used for tensile testing.

The tensile tests were conducted at the Emerging Materials Research Unit (EMRU), Ferhat Abbas Sétif 1 University using an MTS apparatus equipped with a 50 kN force sensor at room temperature (Figure 5).

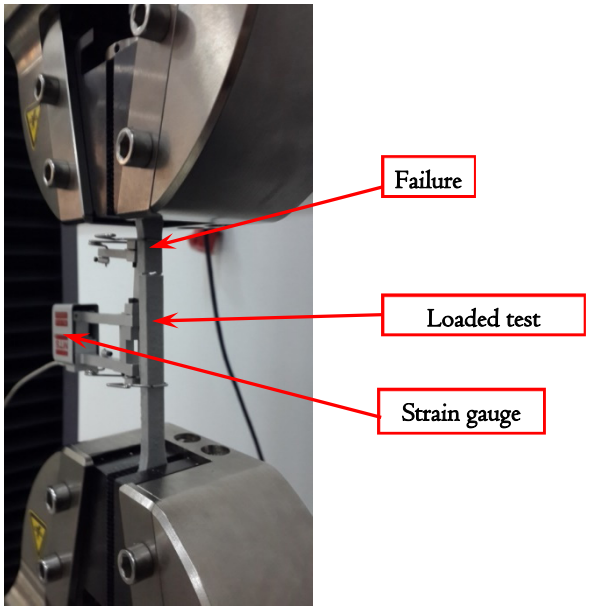

Figure 5. Tensile test setup.

Adhesion tests were conducted on composite plates bonded with resin to determine adhesion properties between CFRP and resin (Figure 6). The tests were conducted using an MTS universal testing machine equipped with a 50 kN load cell, maintaining a constant crosshead speed of 1 mm/min.

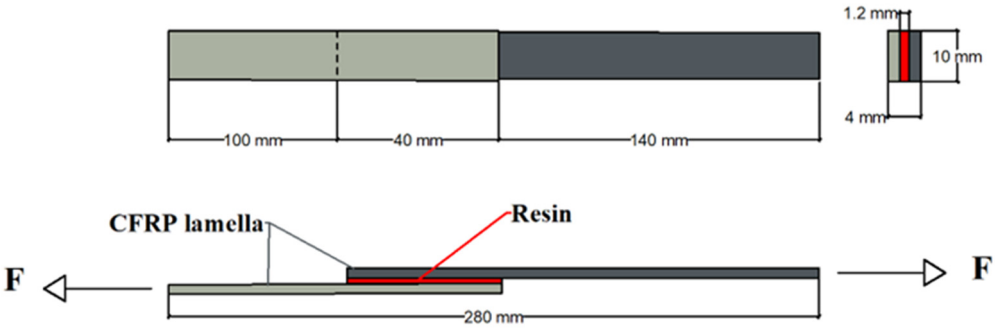

Figure 6. Resin–composite adhesion test.

Six concrete blocks were prepared for the pull-out tests using a mix with a water-to-cement ratio (W/C) of 0.61, formulated according to the Dreux–Gorisse method [34]. The concrete composition and its mechanical characteristics are in Table 6. The blocks were cast, cured for 28 days, and then prepared for testing by creating grooves to accommodate the CFRP strips.

Table 6. Concrete composition.

Composition	Quantity
Sand 0/3 (kg/m^3)	682.59
Gravel 3/8 (kg/m^3)	125.10
Gravel 8/15 (kg/m^3)	357.42
Gravel 15/25 (kg/m^3)	357.42
Cement (m^3)	350
Water (L/m^3)	215

The concrete mechanical characteristics are in Table 7.

Table 7. Concrete mechanical characteristics.

	Average Compressive Strength (MPa)	Average Tensile Strength (MPa)	Average Young's Modulus (GPa)
Values	30.5	3.3	29.7
S.D (MPa)	1.32	0.2	1.47
C.V (%)	4	6	5

S.D: Standard deviation; C.V: Coefficient of Variation.

The reinforcements used for the pull-out test are CFRP lamellas, whose mechanical properties are in Table 8.

Table 8. The mechanical properties of the CFRP lamella.

Reinforcement Type	Width (mm)	Thickness (mm)	Yield Strength (MPa)	Young's Modulus (GPa)
CFRP lamella	10	1.4	2500	205

Concrete blocks (75 × 75 × 250 mm^3) were cast (Figure 7a) and covered with a plastic sheet for 24 h. Subsequently, the prisms were placed in a water tank for 27 days for curing. After the curing, they were removed from the water tank and grooved with a concrete saw (Figure 7b). Then, concrete blocks were kept one more day for assuring a dry surface. The anchorage length was set to 120 mm, with 50 mm left unbonded at the loaded end to prevent edge failure. A 100 mm length of the FRP lamella extended outside the cement block and was attached to steel plates (50 × 35 × 1) to facilitate load application. The FRP lamellas were centered in the grooves to prevent adhesive material from occupying unwanted areas (Figure 7c).

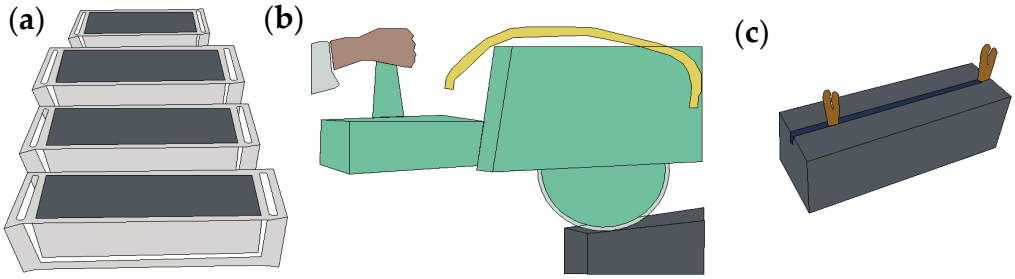

Figure 7. Sample preparation. (**a**) concrete prism casting; (**b**) grooving; (**c**) installation of the CFRP strips in the center of the groove.

Table 9 provides detailed information about the samples used in these tests.

Table 9. Pull-out samples.

Sample Name	Type of Resin	Embedment Length	Reinforcement Type	Reinforcement Dimensions	Groove Size (mm)
Block 1	Mixture 1	100 mm	CFRP	1.4 × 10	5 × 15
Block 2	Mixture 3				

The pull-out procedure in our study closely follows that of Al-Saadi et al. [20]. Monotonic load application was conducted using an MTS universal testing machine, Equation (2).

$$\sigma_{max}\text{moy} = \frac{F_{max}moy}{2 \times w_f \times L_b} \quad (2)$$

where

- F_{max}moy: average maximum pull-out force (kN).
- σ_{max}moy: average pull-out stress (MPa).
- W_f and L_b: width of the plate and bond length, respectively.
- Pu: predicted pull-out force (kN).

Finally, the pull-out forces obtained from the experimental tests were compared with theoretical predictions using a static model. Numerous empirical and fracture mechanics models are available to predict the pull-out force of FRP bars [7]. However, few theoretical models can predict the pull-out force of FRP bars embedded in concrete using the Near Surface Mounted (NSM) technique. In this study, a static model was adopted to predict the ultimate load (Pu), according to Equation (3) [20]:

$$Pu = \alpha \times \beta \times \sqrt{fc} \times dp^{1.36} \times bp^{0.21} \quad (3)$$

where α is a characteristic value to account for the influence of the surface type (i.e., smooth or rough) and the dimensions of the CFRP lamella: α equals 0.23 for 1.4 × 10 mm smooth CFRP lamellas and 0.25 for 1.4 × 10 mm rough CFRP lamellas; fc is the concrete compressive strength at 28 days; β is the ratio between the anchorage length and 200; dp is the lamella width; and bp is the lamella thickness.

3. Result and Discussion

Through rigorous testing, the efficacy of the epoxy resin in enhancing the structural integrity, durability, and chemical resistance of treated cementitious materials was assessed. Table 10 lists the density results.

Table 10. Resin Density.

	Density (g/cm^3)			Average (g/cm^3)	S.D (g/cm^3)	C.V (%)
Mixture 1	1.397	1.507	1.551	1.485	0.079	5
Mixture 2	1.522	1.614	1.406	1.514	0.104	7
Mixture 3	1.618	1.608	1.496	1.574	0.068	4
Mixture 4	1.616	1.701	1.495	1.604	0.104	6

S.D: Standard Deviation; C.V: Coefficient of Variation.

The observed increase in density with a higher silica content is attributed to the inherent density of the silica particles (approximately 2.7 g/cm^3), which is significantly higher than that of the epoxy resin (1.3 g/cm^3). This relationship highlights the direct impact of the filler content on the physical properties of composite materials, demonstrating how incorporating sand can modify and enhance the final product's characteristics. Figure 8 shows the stress–strain diagrams for the mixtures.

The tensile tests revealed that the addition of silica sand improved the tensile strength and Young's modulus of the epoxy resin composites. All mixtures exhibit an elastic behavior and a brittle response. Table 11 summarizes their tensile mechanical properties.

The tensile strength increased from 29.47 MPa in Mixture 1 to 35.52 MPa in Mixture 3. Similarly, the elastic modulus ranges from 4.38 GPa to 5.83 GPa, indicating a substantial enhancement in the material's stiffness. Conversely, the elastic deformation decreases by 38%. The increase in the tensile strength and elastic modulus can be attributed to the improved interfacial bonding between the filler and the epoxy matrix. The angular and rough surface texture of the silica particles contributed to better interlocking and load transfer within the composite. This output complies with previous studies on the mechanical performance of mineral fillers in polymer matrices (RIF). The optimal performance was observed at a 10% silica sand content and beyond the tensile strength slightly decreased (Mixture 4). This reduction may be due to the increased brittleness and reduced elongation at the break (from 8.87% to 5.5%), which indicates a transition from a ductile to a more brittle failure mode. Therefore, only Mixture 1 and Mixture 3 have been investigated in the resin–reinforcement adhesion tests. Table 12 lists the results of the Resin–Reinforcement adhesion tests. The

adhesion strength between the CFRP and the resin was significantly improved with the inclusion of silica sand.

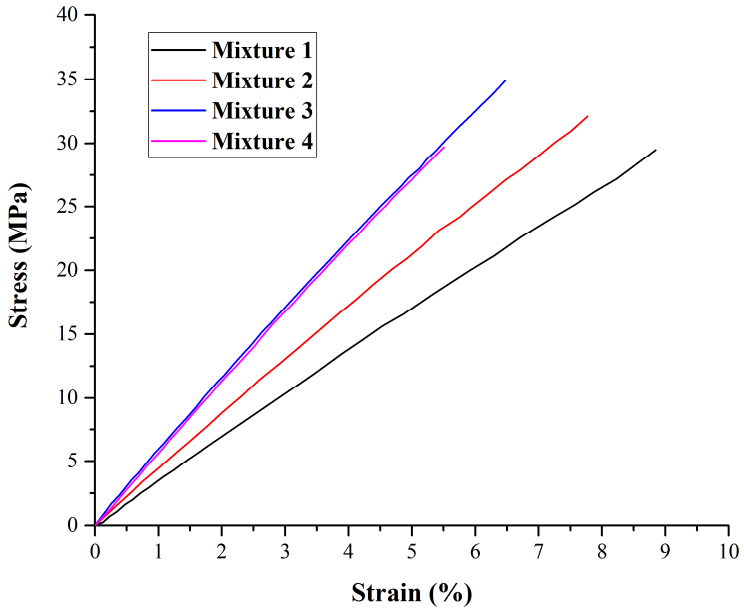

Figure 8. The tensile curve of mixtures.

Table 11. The tensile mechanical properties of mixtures.

Mix	σ_{max} (MPa)	S.D (MPa)	C.V (%)	ε_{rup} (%)	S.D (%)	C.V(%)	E (GPa)	S.D (GPa)	C.V (%)
Mixture 1	29.47	0.60	2.04	8.87	0.13	1.47	4.38	0.16	3.65
Mixture 2	32.82	1.00	3.05	7.93	0.07	0.88	4.92	0.08	1.63
Mixture 3	35.52	0.48	1.35	6.50	0.20	3.08	5.83	0.07	1.20
Mixture 4	31.28	1.48	4.17	5.50	0.20	3.64	5.82	0.18	3.09

S.D: Standard deviation; C.V: Coefficient of Variation.

Table 12. Resin and composite adhesion results.

Sample	Fmax (kN)	Average (kN)	S.D (kN)	C.V (%)
Mixture 1	6.22 5.87 7.03	6.37	0.595	9
Mixture 3	8.54 8.97 9.43	8.97	0.445	5

As shown in Table 12, the average maximum pull-out force increased from 6.37 kN in the unfilled resin (Mixture 1) to 8.97 kN in Mixture 3.

Figure 9 demonstrates the failure mode of the resin–CFRP bond, which is abrupt at the bonded surface. Notably, the resin retains traces of carbon fibers, indicating chemical solid adhesion. Cleaning the carbon reinforcements with acetone enhances the adhesion process, ensuring optimal bonding [6].

Two concrete blocks were cast and subjected to direct pull-out tests to investigate the effect of a sand addition to the resin. Table 13 lists the direct pull-out tests.

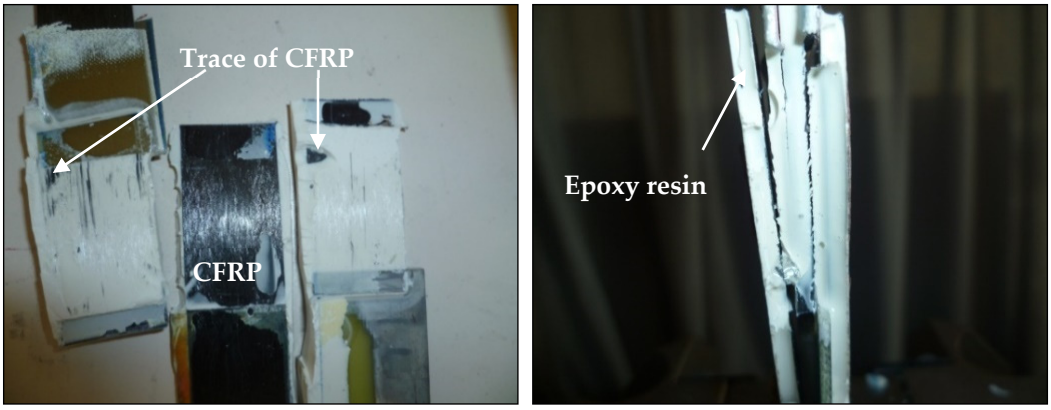

Figure 9. Resin–CFRP rupture type.

Table 13. Direct pull-out results.

Samples	F Max Average (kN)	S Max Average (mm)	σ Max Average (MPa)	Pu (kN)
block 1	14.21	0.38	7.11	15.61
block 2	18.79	0.23	9.40	16.97

The blocks have a comparable behavior of the slip–adhesion curve (Figure 10). In the adhesion force−displacement curves, the ascending section is followed by a descending one. Due to the sand addition, the resin–reinforcement contact surface in block 2 is rougher than in block 1. The maximum pull-out strength of block 2 is higher than block 1 (i.e., 18.79 kN vs. 14.2 kN), demonstrating an increase in the bond strength of approximately 32%.

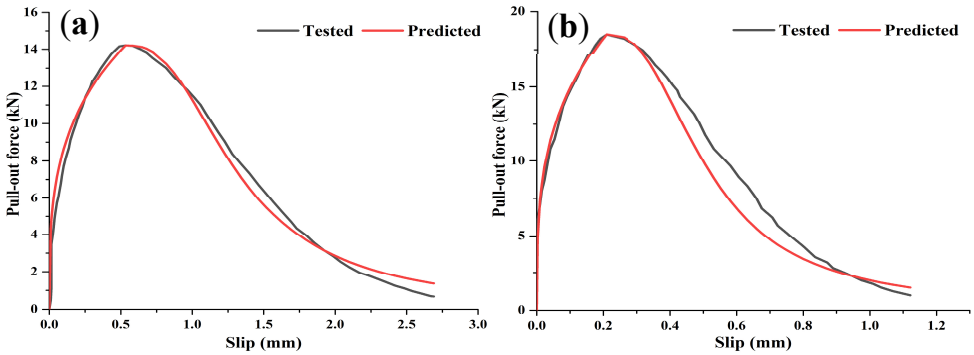

Figure 10. Bond stress vs. loaded-end slip relations of tested specimens: (**a**) block 1 and (**b**) block 2.

In block 1, the failure mode is sliding between CFRP reinforcement and the sealing material without cracks along the anchor length. Conversely, block 2 experiences failure due to concrete crushing surrounded by etching, without evidence of sliding on the reinforcement. The shift in the failure mode suggests that the resin with silica sand filler provides better mechanical interlocking and stress distribution, reducing the likelihood of premature debonding and enhancing the overall structural integrity. The increased pull-out force and the reduced slip at the maximum load indicate a more robust and reliable bond between the CFRP and the concrete, which is critical for the long-term performance of repaired structures.

The bond-slip behavior of CFRP and the residual strength of concrete are critically dependent on the mode of failure and the failure status. Initially, the bond between CFRP and concrete is dominated by the adhesion between the epoxy resin and the concrete, exhibiting a linear bond–slip relationship [35]. As the loading increases, micro-cracks form, introducing non-linearity due to enhanced mechanical interlocking from surface

roughness [36]. In the macro-cracking phase, bond stress significantly decreases, with failure modes including concrete shear failure (block 2) characterized by a sudden drop in the bond stress and interface debonding, marked by a gradual stress reduction (block 1).

Surface treatment techniques and consistent quality control are essential to achieve the desired roughness levels and maximize the bond performance [37]. The roughness of both CFRP bars and the grooves significantly influences the bond behavior in NSM-CFRP systems by enhancing mechanical interlocking and adhesion [37]. Increased roughness at the CFRP–resin interface improves mechanical interlocking and frictional resistance, reducing slip and enhancing the load transfer efficiency [38]. Similarly, a rougher groove–resin interface increases mechanical interlocking and the adhesive bond strength between the epoxy resin and concrete, preventing debonding and ensuring secure anchorage [39]. The combined roughness of the CFRP bars and grooves creates a synergistic effect, optimizing the load distribution, reducing the risk of localized failures, and enhancing the long-term performance and durability of the NSM-CFRP system [40]. Aiello et al. [41] demonstrated that the highest shear stress values, around 18 MPa, occur with roughened surfaces, leading to concrete failure, whereas smoother surfaces result in bar–concrete interface failure with lower maximum shear stress of around 4 MPa.

According to Equation (3), in this study, α is 0.25 for block 2 and 0.23 for block 1. The predicted pullout force values (Pu) compared to the experimental pullout force (fmax) are in Table 13. The comparison between the experimental and theoretical pull-out forces confirmed the validity of the model for predicting the bond strength of the NSM CFRP system, highlighting the effectiveness of the silica-filled epoxy resin in enhancing the bond performance.

Studying the bond–slip relationship is crucial for evaluating the bond capacity of members adjacent to cracks, where local strain compatibility between the bar and surrounding concrete is critical. The bond–slip curve of the NSM CFRP bars is analyzed using the equation employed by Douadi et al. [17] to determine the bond–slip characteristics between the reinforcing bars and the surrounding concrete.

$$\text{Ascendant}: \quad \tau_{av} = \tau_u \left(\frac{S}{S_u} \right)^a \tag{4}$$

$$\text{Downgrade}: \quad \tau_{av} = \tau_u \frac{\frac{S}{S_u}}{b\left(\frac{S}{S_u} - 1\right)^3 + \frac{S}{S_u}} \tag{5}$$

where τ_{av} is the average bond stress of the NSM CFRP bar.

- S: is the slipping NSM CFRP bar.
- τ_u is the bond strength at the maximum load.
- S_u is the slipping at the maximum load.
- a and b are parameters of ascendant and downgrade of the bond stress–slip curve, respectively.

The comparisons between τu calculated using Equations (4) and (5) for both ascending and descending branches, and the experimental results for the two configurations (Block 1 block and 2), are depicted in the figure. Figure 10 illustrates that the predicted curves align well with the experimental data from the specimens.

4. Conclusions

The incorporation of silica sand into epoxy resin composites significantly improved the mechanical and adhesion properties, highlighting its potential for enhancing CFRP–concrete bonding in structural applications. The composite material comprises a matrix enveloping a filler, with each component fulfilling a distinct role in the material's mechanical behavior. The matrix acts as a binder, bearing all stresses, distributing forces, and safeguarding the reinforcement. Meanwhile, the filler introduces novel properties to the matrix. The interaction between the matrix and the filler, as demonstrated through the

enhanced mechanical and adhesion properties, underscores the effectiveness of silica sand in the composite structure. The detailed analysis of these components reveals the following key findings:

- The addition of silica sand to the epoxy resin resulted in a noticeable increase in the density of the composite material. This aligns with findings from other studies that highlight the impact of high-density fillers on composite materials, thereby enhancing their structural integrity and resistance to deformation.
- Tensile tests showed that the optimal addition of silica sand (10%) to the epoxy resin significantly improved its tensile strength and elastic modulus. The tensile strength increased from 29.47 MPa for unfilled resin to 35.52 MPa, and the elastic modulus rose from 4.38 GPa to 5.83 GPa. These enhancements can be attributed to the effective mechanical interlocking and improved load transfer provided by the silica particles, which confirms previous research on mineral fillers in polymer composites.
- Adhesion tests between CFRP and the resin composites revealed a substantial increase in the pull-out force, from 6.37 kN in the unfilled resin to 8.97 kN in the resin with 10% silica sand. This improvement highlights the effectiveness of silica fillers in enhancing the bond strength by increasing surface roughness and providing better mechanical interlocking, which is critical for the long-term durability of repaired structures.
- This study identified that a 10% silica sand content provided the best balance between strength and ductility, improving the mechanical properties and the bond strength without significantly compromising the material's flexibility. Beyond this percentage, the material exhibited increased brittleness, which could reduce its effectiveness in certain applications.
- The direct pull-out tests on concrete blocks demonstrated that the silica-filled resin significantly improved the bond strength between CFRP and concrete, increasing the maximum pull-out force from 14.21 kN to 18.79 kN. This finding supports the use of silica-filled epoxy resin as a cost-effective and efficient solution for enhancing the performance of CFRP–concrete bonds in structural applications.
- The inclusion of silica sand shifted the failure mode from adhesive debonding to concrete crushing, indicating a stronger bond and better load distribution across the composite material. This shift is critical for ensuring the durability and reliability of reinforced concrete structures subjected to high loads.
- The adopted analytical models align closely with the experimentally observed bond stress–slip relationship for CFRP lamella.

While the innovative use of silica-filled epoxy resin composites offers a promising avenue for advancing the performance and sustainability of CFRP–concrete bonding systems in civil engineering, future research should explore:

- The long-term durability of these composites under various environmental conditions, such as moisture, temperature fluctuations, and chemical exposure.
- The optimization of filler particle size and distribution to further enhance the mechanical properties and adhesion strength.
- The application of other mineral fillers and their potential synergistic effects with silica sand to develop more advanced composite materials.

Author Contributions: Data curation, formal analysis, investigation, methodology: all authors; Writing—original draft: R.B., K.H., A.D., M.B., R.H., S.D., G.D.S. and L.M.; Writing—review and editing: K.H., A.D., G.D.S. and L.M. All authors contributed equally to this paper. All authors have read and agreed to the published version of the manuscript.

Funding: This research received no external funding.

Institutional Review Board Statement: Not applicable.

Informed Consent Statement: Not applicable.

Data Availability Statement: The data presented in this study are available on request from the corresponding author. The data are not publicly available due to privacy reason.

Acknowledgments: The authors acknowledge the support from the Directorate-General for Scientific Research and Technological Development (DGRSDT-Algeria). The authors are grateful to Merdas Abdelghani and Benrebouh Imed (Department of Civil Engineering, University of Ferhat Abbas, Sétif, Algeria) for their help to conduct the experimental program at Emerging Materials Research Unit (EMRU).

Conflicts of Interest: The authors declare no conflicts of interest.

References

1. Abed, M.A.; Alkurdi, Z.; Fořt, J.; Černý, R.; Solyom, S. Bond behavior of FRP bars in lightweight SCC under direct pull-out conditions: Experimental and numerical investigation. *Materials* **2022**, *15*, 3555. [CrossRef] [PubMed]
2. Hegde, S.; Shenoy, B.S.; Chethan, K. Review on carbon fiber reinforced polymer (CFRP) and their mechanical performance. *Mater. Today Proc.* **2019**, *19*, 658–662. [CrossRef]
3. Capozucca, R. Damage to reinforced concrete due to reinforcement corrosion. *Constr. Build. Mater.* **1995**, *9*, 295–303. [CrossRef]
4. Hosen, M.A.; Jumaat, M.Z.; Alengaram, U.J.; Islam, A.S.; Bin Hashim, H. Near surface mounted composites for flexural strengthening of reinforced concrete beams. *Polymers* **2016**, *8*, 67. [CrossRef] [PubMed]
5. Al-Mahmoud, F.; Castel, A.; François, R.; Tourneur, C. Strengthening of RC members with near-surface mounted CFRP rods. *Compos. Struct.* **2009**, *91*, 138–147. [CrossRef]
6. Parretti, R.; Nanni, A. Strengthening of RC members using near-surface mounted FRP composites: Design overview. *Adv. Struct. Eng.* **2004**, *7*, 469–483. [CrossRef]
7. Chen, J.F.; Teng, J. Anchorage strength models for FRP and steel plates bonded to concrete. *J. Struct. Eng.* **2001**, *127*, 784–791. [CrossRef]
8. Yu, J.-G.; Cheng, L.; Shen, X.; Hu, Y.; Li, B. Flexural performance of RC beams strengthened with inorganic adhesive bonded NSM CFRP bar. *Structures* **2022**, *44*, 1025–1035. [CrossRef]
9. Merdas, A.; Fiorio, B.; Chikh, N.-E. Composites, Aspects of bond behavior for concrete beam strengthened with carbon fibers reinforced polymers–near surface mounted. *J. Reinf. Plast. Compos.* **2015**, *34*, 463–478. [CrossRef]
10. Szewczak, A. Influence of epoxy glue modification on the adhesion of CFRP tapes to concrete surface. *Materials* **2021**, *14*, 6339. [CrossRef]
11. Li, C.; Ke, L.; He, J.; Chen, Z.; Jiao, Y. Effects of mechanical properties of adhesive and CFRP on the bond behavior in CFRP-strengthened steel structures. *Compos. Struct.* **2019**, *211*, 163–174. [CrossRef]
12. Soares, S.; Sena-Cruz, J.; Cruz, J.R.; Fernandes, P. Influence of surface preparation method on the bond behavior of externally bonded CFRP reinforcements in concrete. *Materials* **2019**, *12*, 414. [CrossRef] [PubMed]
13. Shield, C.; French, C.; Milde, E. The effect of adhesive type on the bond of NSM tape to concrete. In Proceedings of the 7th International Symposium on Fiber-Reinforced (FRP) Polymer Reinforcement for Concrete Structures, Kansas City, MO, USA, 6–9 November 2005; Volume 230, pp. 355–372.
14. Sharaky, I.A.; Torres, L.; Comas, J.; Barris, C. Flexural response of reinforced concrete (RC) beams strengthened with near surface mounted (NSM) fibre reinforced polymer (FRP) bars. *Compos. Struct.* **2014**, *109*, 8–22. [CrossRef]
15. Lee, D.; Cheng, L.; Hui, J.Y.-G. Bond characteristics of various NSM FRP reinforcements in concrete. *J. Compos. Constr.* **2013**, *17*, 117–129. [CrossRef]
16. Boutlikht, M.; Lahbari, N.; Hebbache, K.; Tabchouche, S. The assessment of strips arrangement effect on the performance of strengthened reinforced concrete beams. *J. Adhes. Sci. Technol.* **2022**, *36*, 1510–1527. [CrossRef]
17. Douadi, A.; Merdas, A.; Sadowski, Ł. The bond of near-surface mounted reinforcement to low-strength concrete. *J. Adhes. Sci. Technol.* **2019**, *33*, 1320–1336. [CrossRef]
18. Sadoun, O.; Merdas, A.; Douadi, A. The bond and flexural strengthening of reinforced concrete elements strengthened with near surface mounted prestressing steel (PS) bars. *J. Adhes. Sci. Technol.* **2020**, *34*, 2120–2143. [CrossRef]
19. Benedetti, A.; Fernandes, P.; Granja, J.L.; Sena-Cruz, J.; Azenha, M. Influence of temperature on the curing of an epoxy adhesive and its influence on bond behaviour of NSM-CFRP systems. *Compos. Part B Eng.* **2016**, *89*, 219–229. [CrossRef]
20. Al-Saadi, N.T.K.; Al-Mahaidi, R.; Abdouka, K. Bond behaviour between NSM CFRP strips and concrete substrate using single-lap shear testing with cement-based adhesives. *Aust. J. Struct. Eng.* **2016**, *17*, 28–38. [CrossRef]
21. Mohammed, A.; Al-Saadi, N.T.K.; Al-Mahaidi, R. Bond behaviour between NSM CFRP strips and concrete at high temperature using innovative high-strength self-compacting cementitious adhesive (IHSSC-CA) made with graphene oxide. *Constr. Build. Mater.* **2016**, *127*, 872–883. [CrossRef]
22. Rahman, M.M.; Jumat, M.Z.; Hosen, M.A.; Islam, A.S. Effect of adhesive replacement with cement mortar on NSM strengthened RC Beam. *J. Constr.* **2016**, *15*, 61–72. [CrossRef]
23. Torres, L.; Sharaky, I.A.; Barris, C.; Baena, M. Experimental study of the influence of adhesive properties and bond length on the bond behaviour of NSM FRP bars in concrete. *J. Civ. Eng. Manag.* **2016**, *22*, 808–817. [CrossRef]

24. Mohammed, A.; Al-Saadi, N.T.; Al-Mahaidi, R. Assessing the contribution of the CFRP strip of bearing the applied load using near-surface mounted strengthening technique with innovative high-strength self-compacting cementitious adhesive (IHSSC-CA). *Polymers* **2018**, *10*, 66. [CrossRef] [PubMed]
25. Al-Saadi, N.T.K.; Mohammed, A.; Al-Mahaidi, R. Bond performance of NSM CFRP strips embedded in concrete using direct pull-out testing with cementitious adhesive made with graphene oxide. *Constr. Build. Mater.* **2018**, *162*, 523–533. [CrossRef]
26. Cruz, J.R.; Sena-Cruz, J.; Rezazadeh, M.; Seręga, S.; Pereira, E.; Kwiecień, A.; Zając, B. Bond behaviour of NSM CFRP laminate strip systems in concrete using stiff and flexible adhesives. *Compos. Struct.* **2020**, *245*, 112369. [CrossRef]
27. Mohammadi-Firouz, R.; Pereira, E.N.; Barros, J.A. Experimental assessment of the thermo-mechanical bond behavior of NSM CFRP with cement-based adhesives. *Constr. Build. Mater.* **2023**, *364*, 129980. [CrossRef]
28. Bondioli, F.; Darecchio, M.E.; Luyt, A.S.; Messori, M. Epoxy resin modified with in situ generated metal oxides by means of sol–gel process. *J. Appl. Polym. Sci.* **2011**, *122*, 1792–1799. [CrossRef]
29. Irekti, A. Boumerdes, Synthèse des matériaux composites à matrice thermodurcissable et charge minérale. *Mémoire Magister Boumerdes* **2011**, *110*, 49–53.
30. Fu, S.-Y.; Feng, X.-Q.; Lauke, B.; Mai, Y.-W. Effects of particle size, particle/matrix interface adhesion and particle loading on mechanical properties of particulate–polymer composites. *Compos. Part B Eng.* **2008**, *39*, 933–961. [CrossRef]
31. Laouchedi, D.; Bezzazi, B.; Aribi, C. Elaboration and characterization of composite material based on epoxy resin and clay fillers. *J. Appl. Res. Technol.* **2017**, *15*, 190–204. [CrossRef]
32. *NF T 51-561*; Plastiques—Détermination de la Masse Volumique en Fonction de la Température—Méthode par Immersion. Association Française de Normalisation: Paris, France, 1990.
33. *ISO 527-2:2012*; Plastics-Determination of Tensile Properties-Part 2: Test Conditions for Moulding and Extrusion Plastics. International Organization for Standardization: Geneva, Switzerland, 2012.
34. George, D.; Jean, F. *Nouveau Guide du Béton et de Ses Constituants [New Guide of Concrete and Its Constituents]*; Eyrolles: Paris, France, 1998.
35. Zeng, J.-J.; Liao, J.; Zhuge, Y.; Guo, Y.-C.; Zhou, J.-K.; Huang, Z.-H.; Zhang, L. Bond behavior between GFRP bars and seawater sea-sand fiber-reinforced ultra-high strength concrete. *Eng. Struct.* **2022**, *254*, 113787. [CrossRef]
36. Peng, K.-D.; Zeng, J.-J.; Huang, B.-T.; Huang, J.-Q.; Zhuge, Y.; Dai, J.-G. Bond performance of FRP bars in plain and fiber-reinforced geopolymer under pull-out loading. *J. Build. Eng.* **2022**, *57*, 104893. [CrossRef]
37. Sharaky, I.A.; Torres, L.; Baena, M.; Miàs, C. An experimental study of different factors affecting the bond of NSM FRP bars in concrete. *Compos. Struct.* **2013**, *99*, 350–365. [CrossRef]
38. Lee, D.; Cheng, L. Bond of NSM systems in concrete strengthening–examining design issues of strength, groove detailing and bond-dependent coefficient. *Constr. Build. Mater.* **2013**, *47*, 1512–1522. [CrossRef]
39. Garzón-Roca, J.; Sena-Cruz, J.M.; Fernandes, P.; Xavier, J. Effect of wet-dry cycles on the bond behaviour of concrete elements strengthened with NSM CFRP laminate strips. *Compos. Struct.* **2015**, *132*, 331–340. [CrossRef]
40. Ariyachandra, M.; Gamage, J.; Al-Mahaidi, R.; Kalfat, R. Effects of surface roughness and bond enhancing techniques on flexural performance of CFRP/concrete composites. *Compos. Struct.* **2017**, *178*, 476–482. [CrossRef]
41. Antonietta Aiello, M.; Leone, M.; Pecce, M. Bond performances of FRP rebars-reinforced concrete. *J. Mater. Civ. Eng.* **2007**, *19*, 205–213. [CrossRef]